

## Shooting method applied to porous rotating disk: Darcy-Forchheimer flow of nanofluid

Muzamal Hussain\*<sup>1</sup>, Humaira Sharif<sup>1</sup>, Mohamed A. Khadimallah<sup>2</sup>, Abir Mouldi<sup>3</sup>,  
Hassen Loukil<sup>4</sup>, Mohamed R. Ali<sup>5,6</sup> and Abdelouahed Tounsi<sup>7,8</sup>

<sup>1</sup>Department of Mathematics, Govt. College University Faisalabad, 38000, Faisalabad, Pakistan

<sup>2</sup>Prince Sattam Bin Abdulaziz University, College of Engineering, Civil Engineering Department, BP 655, Al-Kharj, 11942, Saudi Arabia

<sup>3</sup>Department of Industrial Engineering, College of Engineering, King Khalid University, Abha – 61421, Kingdom of Saudi Arabia

<sup>4</sup>Department of Electrical Engineering, College of Engineering, King Khalid University, Abha – 61421, Saudi Arabia

<sup>5</sup>Faculty of Engineering and Technology, Future University in Egypt New Cairo 11835, Egypt Basic Engineering Science

<sup>6</sup>Department, Benha Faculty of Engineering, Benha University, Benha, Egypt

<sup>7</sup>YFL (Yonsei Frontier Lab), Yonsei University, Seoul, Korea

<sup>8</sup>Department of Civil and Environmental Engineering, King Fahd University of Petroleum and Minerals,  
31261 Dhahran, Eastern Province, Saudi Arabia

(Received January 31, 2021, Revised November 18, 2022, Accepted December 7, 2022)

**Abstract.** The characteristics of motile microorganism and three dimensional Darcy-Forchheimer nanofluid flow by a porous rotatable disk with heat generation/absorption is reported. Thermophoretic and Brownian motion aspects are included by utilizing Buongiorno model. Moreover, slip conditions are considered on velocity, thermal, concentration and microorganism. Shooting procedure is implemented to find the numerical results of physical quantities are evaluated parametrically. The different physical parameters like heat sink/source parameter, thermal, Brownian number, thermophoresis parameter, concentration, Peclet number, bioconvected Lewis number, microorganism on concentration and density of motile microorganism distributions is considered. Graphs of concentration and microorganism are plotted to examine the influence of distinct prominent flow parameters.

**Keywords:** bioconvected Lewis number; heat generation/absorption; microorganism; peclet number; shooting method

### 1. Introduction

Latest advancement in field of fluid dynamics has taken nanofluid under consideration which shows large thermal conductance and enlarges property of heat transformation in fluids. With quick advancement in technology, the challenges for increasing efficiency of energy exchanger and techniques for saving of energy are being met with the use of new materials. Moreover, conventional heat exchanger fluids could not meet exclusive conditions such as stable intensity of heat exchanger. Nanofluids contain the nano-size particles suspended in fluidic surface and the size of particles is less than 100nm. Nanoliquids have huge thermo-physical characteristics like viscosity, thermal conductivity and coefficient of heat exchanger in comparison to their base liquids. Thermal conductivity is basic feature of nanoliquids. Nanoliquids have great applications in different fields of technology and science. In addition, nanoliquids with special purpose are utilized in heat transfer devices, enhancing the efficiency of diesel generators, treatment of tumor, cooling/warming of home appliances and so on. The production of energetic nano-liquids with controlling micro framework is feasible because of chemical

procedure. This is helpful to construct the micro framework which can make to control the chemical reactions that take place at a high speed and include a high degree of accuracy. Firstly, Wang 1988 studied the fluid behavior along the stretching cylinder. The detailed study of fluid flow along the stretched cylinder for the boundary layer was made (Ishak and Nazar 2009) regarding. Wang 2011 obtained asymptotic solutions for high Reynold number using slip flow condition. Mixed convection condition together with slip flow and obtained numerical solution for the boundary layer problem of Williamson fluid flow over a stretching cylinder (Salahuddin *et al.* 2017). Akbaş (2016a, b) studied the forced vibration analysis of a simple supported viscoelastic nanobeam based on modified couple stress theory (MCST). The nanobeam is excited by a transverse triangular force impulse modulated by a harmonic motion. The elastic medium is considered as Winkler-Pasternak elastic foundation. The damping effect is considered by using the Kelvin-Voigt viscoelastic model. The cracked beam is modelled using a proper modification of the classical cracked-beam theory consisting of two sub-beams connected through a massless elastic rotational spring. Khan *et al.* (2022) investigated the free convection flow of Prabhakar fractional Jeffrey fluid on an oscillated vertical plate with homogenous heat flux. With the help of the Laplace transform and the Boussinesq's approximation, precise solutions for dimensionless momentum may be found.

\*Corresponding author, Ph.D.,

E-mail: muzamal45@gmail.com;

muzamalhussain@cuf.edu.pk

The temperature and velocity of Prabhakar fractional time free convection flows are compared to conventional thermal transport, as shown by Fourier's law. The effects of Soret and Dufour for the Casson fluid by considering the heat transfer along stretching cylinder was worked out (Mahdy, 2015). The mass and convective heat conditions for Casson fluid flow having nanoparticles along stretching cylinder was presented (Maria *et al.* 2016). A thorough numerical study of sisko fluid flow over stretching cylinder with effects of thermal conductivity and viscous dissipation was done (Malik *et al.* 2016). Al-Maliki *et al.* (2020) carried out the dynamic analysis of functionally graded (FG) graphene-reinforced beams under thermal loading based on finite element approach. The presented formulation is based on a higher order refined beam element accounting for shear deformations. The graphene-reinforced beam is exposed to transverse periodic mechanical loading. Akbaş (2017a, b) investigated the free vibration analysis of edge cracked cantilever microscale beams composed of functionally graded material (FGM) based on the modified couple stress theory (MCST). The material properties of the beam are assumed to change in the height direction according to the exponential distribution. The FG nanobeam is excited by a transverse triangular force impulse modulated by a harmonic motion. Mechanical properties of FG beam depends on the position. The Kelvin–Voigt model is considered in the damping effect. In solution of the dynamic problem, finite element method is used within Timoshenko beam theory. Sun *et al.* (2022) explored the sequel to the biocompatibility, physico-chemical properties, high electrical conduction of copper nanoparticles over an inclined surface, little is known on the significance of nanoparticle radius, and inclined magnetic field on the dynamics of chemical reactive water conveying copper nanoparticles through a porous medium in the presence of Joule heating and spacing heating. In this case, there exists convective heating of the inclined surface due to thermal and significant concentration at the wall. The uniform suction/blowing effects together with transfer of heat outside the permeable stretching cylinder were considered (Ishaq *et al.* 2008). Under convective boundary conditions, electrically conducting sisko fluid along the stretching cylinder in axial direction was probed (Khan and Malik 2015). They found the considerable boost in the flow parameters for shear thinning than thickening. The notable point about all the above mentioned studies is that the considered fluid is “Pure”. Practically it is almost impossible to have such fluid which is free from any kind of impurity. Every naturally occurring fluid contains dust particles. Many engineering and industrial problems deal with dusty fluid such as powder mechanization and centrifugal technique to the detachment of particles from the fluid. Flow of dusty fluid can be viewed in many natural phenomena e.g. flow of mud in rivers, blood flow and atmospheric flow during haze. Initiative study of motion of dust particles in laminar flow has been carried out (Saffman 1962). An analysis for viscous, incompressible steady flow of dusty fluid flowing between two co-axial rotating cylinders under pressure gradient effect was carried out (Girishwar 1970). Akbaş (2018) investigated the forced vibration analysis of a cracked functionally graded

microbeam using modified couple stress theory with damping effect. Mechanical properties of the functionally graded beam change vary along the thickness direction. The crack is modelled with a rotational spring. The Kelvin-Voigt model is considered in the damping effect. static bending of an edge cracked cantilever nanobeam composed of functionally graded material (FGM) subjected to transversal point load at the free end of the beam is investigated based on modified couple stress theory. Material properties of the beam change in the height direction according to exponential distributions. Dawar *et al.* (2022) presented the energy resources are among the essential objectives for the economic advancement of any developed country. Alternatively, fossil fuels that meet a large percentage of the world's energy needs are becoming increasingly rare and their quantity is dwindling. Solar systems which convert solar radiation into useable heat or electricity now play a vital part in the production of renewable energies. Akgoz and Civalek (2011) investigated geometrically the nonlinear free vibration analysis of thin laminated plates resting on non-linear elastic foundations. Winkler-Pasternak type foundation model is used. Governing equations of motions are obtained using the von Karman type nonlinear theory. The method of discrete singular convolution is used to obtain the discretised equations of motion of plates. Batou *et al.* (2019) studied the wave propagations in sigmoid functionally graded (S-FG) plates using new Higher Shear Deformation Theory (HSDT) based on two-dimensional (2D) elasticity theory. The current higher order theory has only four unknowns, which mean that few numbers of unknowns, compared with first shear deformations and others higher shear deformations theories and without needing shear corrector. Sabu *et al.* (2021) proposed the numerical exploration of the hydromagnetic alumina–water nanoliquid flow due to a rotating rigid disk. The nanoliquid flow considering different nanoparticle shapes (namely sphere, platelet, cylinder, and brick) and the thermo-hydrodynamic slip constraints have been modeled utilizing the two-phase modified Buongiorno model (MBM). Baaskaran *et al.* (2018) studied the reliable and accurate method of computationally aided design processes of advanced thin walled structures in automotive industries for the efficient usage of smart materials, that possess higher energy absorption in dynamic compression loading. The most versatile components i.e., thin walled crash tubes with different geometrical profiles are introduced in view of mitigating the impact of varying cross section in crash behavior and energy absorption characteristics. Dusty gas flow in a region occupied by boundary layer was examined (Chakrabarti, 1974). The coefficient of friction and heat transfer for dusty boundary layer flow with pressure gradient was studied (Agranat 1988). Ramesh *et al.* (2022) studied the interaction of nanoparticles with fluids with considerable interest in the area of nanotechnology research. The purpose of this research is to see how a ternary nanofluid performs over a slippery surface. The energy equation is used to explain the heat source/sink effect. As a novel feature of the article, suction, slip effect, and convective boundary conditions are incorporated at the wall.

In addition to these studies for flow and transfer of heat

for dusty fluid along sheet / surface, many researchers considered dusty fluid flow along cylinder. The viscous, incompressible gas flow having dust particles for an isothermal cylinder was discussed and results from various physical parameters were presented (Rebhi 2010). Chen *et al.* (2019a, b) carried the energy absorption characteristics of a lattice-web reinforced composite sandwich cylinder (LRCS) which is composed of glass fiber reinforced polymer (GFRP) face sheets, GFRP lattice webs, polyurethane (PU) foam and ceramsite filler. The vortex-induced vibration of three circular cylinders (each of diameter  $D$ ) in an equilateral triangular arrangement is investigated using the immersed boundary method. Abdulrazzaq *et al.* (2020) investigated the thermo-elastic buckling of small scale functionally graded material (FGM) nano-size plates with clamped edge conditions rested on an elastic substrate exposed to uniformly, linearly and non-linearly temperature distributions employing a secant function based refined theory. Material properties of the FGM nano-size plate have exponential gradation across the plate thickness. Civalek (2017) investigated the free vibration analysis of conical and cylindrical shells and annular plates made of composite laminated and functionally graded materials (FGMs). Carbon nanotubes reinforced (CNTR) composite case is also taken consideration for FGM. The equations of motion for conical shell are obtained via Hamilton's principle using the transverse shear deformation theory. Some valuable results regarding heat transfer of dusty fluid over a hollow stretching cylinder using multi-step DTM were reported (Rasekh *et al.* 2013). Conduction of dusty fluid flow along stretching cylinder with thermal conductivity and viscosity effects were dealt numerically (Konch and Hazarika, 2017). Derakhshandeh1a *et al.* (2020) investigated the Reynolds number  $Re$  ( $= 50-200$ ) effects on the flows around a single cylinder and the two tandem (center-to-center spacing  $L^* = L/D = 4$ ) cylinders, each of a diameter  $D$ . Vorticity structures, Strouhal numbers, and time-mean and fluctuating forces are presented and discussed. Salah *et al.* (2019) employed a simple four-variable integral plate theory for examining the thermal buckling properties of functionally graded material (FGM) sandwich plates. The proposed kinematics considers integral terms which include the effect of transverse shear deformations. In some fresh attempts, the researchers have pondered over new dimensions of stretching i.e., exponentially stretching cylinder. The detailed study of flow and transfer of heat for hyperbolic tangent fluid over a stretching cylinder exponentially in vertical direction was carried out (Naseer *et al.* 2014). Shadravan *et al.* (2019) performed lateral load testing on seventeen wood wall frames in two sections. Section one included eight tests studying structural foam sheathing of shear walls subjected to monotonic loads following the ASTM E564 test method. Similarity solution has been derived for steady boundary layer and heat flow of Casson nanofluid (Malik *et al.* 2013) while cylinder was stretching exponentially along its radius. The flow of Micropolar fluid through vertical exponentially stretching cylinder along the axial direction and discussed heat transfer effects, too, were considered (Rehman *et al.* 2015).

Williamson fluid flow along an exponentially stretching cylinder was examined and they found its numerical solution (Iqbal *et al.* 2018). Recently some researcher used different methods for nonlinear modeling (Eltaher *et al.* 2019, Ebrahimi *et al.* 2019, Safaei *et al.* 2019, Shahsavari *et al.* 2019, Benmansour *et al.* 2019).

All the above mentioned studies give us the incentive to work on a new research thought i.e. effects of of heat source/sink for Darcy-Forchheimer three dimensional nanofluid flow with gyrotactic microorganism by rotatable disk via porous media. No such investigation is reported till date. Shooting method is a tool for its numerical achievements. Many physical and mathematical problems yield highly non-linear differential equations and their exact results are not commonly possible. To evaluate such type of equations numerically, one of the powerful method is to obtain the solution of such problems is shooting technique. This technique is simple, elegant and without any difficult discretization approach. One of the exclusive quality of this approach is that missing boundary value conditions can be started by utilizing smart initial guesses. For better accuracy of solution convergence is investigated by utilizing this method. Impact of relevant physical parameters, like like heat sink/source parameter, thermal, Brownian number, thermophoresis parameter, concentration, Peclet number, bioconvected Lewis number, microorganism are studied & shown through plots.

## 2. Mathematical modeling

We investigate 3D steady Darcy-Forchheimer flow of viscous nanofluid through a porous rotatable disk with heat sink/source and motile microorganism. Further slips under deliberation are velocities, concentration, heat and microorganisms. At  $z=0$  disks is rotatable with constant angular velocity  $\Omega$ . The influences of thermophoretic and Brownian diffusion are accounted for. Here  $(u, v, w)$  are the velocities in the directions of increasing  $(r, \phi, z)$  separately.

The governing boundary layer PDE's are

$$\frac{\partial u}{\partial r} + \frac{u}{r} + \frac{\partial w}{\partial z} = 0 \quad (1)$$

$$\begin{aligned} & u \frac{\partial u}{\partial r} - \frac{v^2}{r} + w \frac{\partial u}{\partial z} \\ & = v \left( \frac{\partial^2 u}{\partial r^2} + \frac{1}{r} \frac{\partial u}{\partial r} - \frac{u}{r^2} + \frac{\partial^2 u}{\partial z^2} \right) - \frac{v}{k^*} u - Fu^2 \\ & + \frac{1}{\rho_f} \left[ \rho_f \beta g (1 - C_\infty) (T - T_\infty) - g (\rho_p - \rho_f) (C - C_\infty) \right] \\ & + \frac{1}{\rho_f} \left[ -\gamma g (\rho_m - \rho_f) (n - n_\infty) \right] \end{aligned} \quad (2)$$

$$\begin{aligned} & u \frac{\partial v}{\partial r} + \frac{uv}{r} + w \frac{\partial v}{\partial z} \\ & = v \left( \frac{\partial^2 v}{\partial r^2} + \frac{1}{r} \frac{\partial v}{\partial r} - \frac{v}{r^2} + \frac{\partial^2 v}{\partial z^2} \right) - \frac{v}{k^*} v - Fv^2 \end{aligned} \quad (3)$$

$$u \frac{\partial w}{\partial r} + w \frac{\partial w}{\partial z} = v \left( \frac{\partial^2 w}{\partial r^2} + \frac{1}{r} \frac{\partial w}{\partial r} + \frac{\partial^2 w}{\partial z^2} \right) - \frac{v}{k^*} w - Fw^2 \quad (4)$$

$$u \frac{\partial T}{\partial r} + w \frac{\partial T}{\partial z} = \alpha_m^* \left( \frac{\partial^2 T}{\partial z^2} + \frac{\partial^2 T}{\partial r^2} + \frac{1}{r} \frac{\partial T}{\partial r} \right) + \frac{Q_o}{(\rho c)_f} (T - T_\infty) + \frac{(\rho c)_p}{(\rho c)_f} \left( D_B \left( \frac{\partial T}{\partial z} \frac{\partial C}{\partial z} + \frac{\partial T}{\partial r} \frac{\partial C}{\partial r} \right) + \frac{D_T}{T_\infty} \left( \left( \frac{\partial T}{\partial z} \right)^2 + \left( \frac{\partial T}{\partial r} \right)^2 \right) \right) \tag{5}$$

$$u \frac{\partial C}{\partial r} + w \frac{\partial C}{\partial z} = D_B \left( \frac{\partial^2 C}{\partial z^2} + \frac{\partial^2 C}{\partial r^2} + \frac{1}{r} \frac{\partial C}{\partial r} \right) + \frac{D_T}{T_\infty} \left( \frac{\partial^2 T}{\partial z^2} + \frac{\partial^2 T}{\partial r^2} + \frac{1}{r} \frac{\partial T}{\partial r} \right) \tag{6}$$

$$u \frac{\partial n}{\partial r} + w \frac{\partial n}{\partial z} + \frac{bW_c}{C_\infty} \left[ \frac{\partial}{\partial z} \left( n \frac{\partial C}{\partial z} \right) \right] = D_m^* \left( \frac{\partial^2 n}{\partial z^2} + \frac{\partial^2 n}{\partial r^2} + \frac{1}{r} \frac{\partial n}{\partial r} \right) \tag{7}$$

The mathematical model is subjected to following boundary conditions

$$u = L_1 \frac{\partial u}{\partial z}, w = 0, v = r\Omega + L'_1 \frac{\partial v}{\partial z}, T = T_w + L'_2 \frac{\partial T}{\partial z}, C = C_w + L'_3 \frac{\partial C}{\partial z}, n = n_w + L'_4 \frac{\partial n}{\partial z} \text{ when } z = 0 \tag{8}$$

$$u \rightarrow 0, v \rightarrow 0, T \rightarrow T_\infty, C \rightarrow C_\infty, n \rightarrow n_\infty \text{ when } z \rightarrow \infty \tag{9}$$

Velocity components are  $u, v$  and  $w$  along the directions of  $r, \phi$  and  $z$  respectively,  $\nu = \frac{\mu}{\rho_f}$  depict kinematic viscosity,  $\rho_f$  the density of base liquid,  $\mu$  is dynamic viscosity,  $k^*$  denotes permeability of porous media,  $\alpha_m^* = \frac{k}{(\rho c)_f}$  stands thermal diffusivity,  $k$  the thermal conductivity,  $(\rho c)_f$  is liquid capacity of heat,  $(\rho c)_p$  is effective heat capacity of nano size particles,  $F = \frac{c_b}{r} k^{\frac{1}{2}}$  is non-uniform inertia parameter,  $T$  represents temperature,  $D_B$  the Brownian coefficient,  $D_T$  is thermophoretic factor,  $C$  the nano size particles concentration,  $Q_o$  is heat source/sink factor,  $D_m^*$  is microorganism diffusivity factor,  $W_c$  symbolizes the maximum swimming speed,  $\kappa$  is Boltzmann constant,  $C_w, C_\infty, T_w, T_\infty, n_w$  and  $n_\infty$  denotes the concentration, heat and motile microorganisms which exist at and far away from the surface.  $L_1, L'_1, L_2, L'_2, L_3, L'_3, L_4, L'_4$  denotes the velocities, thermal, concentration and micro-organism slip coefficients.

We introduce the following variables:

$$u = r\Omega f'(\zeta), w = -(2\Omega\nu)^{\frac{1}{2}} f(\zeta), v = r\Omega g(\zeta), \zeta = \left( \frac{2\Omega}{\nu} \right)^{\frac{1}{2}} z \tag{10}$$

$$\theta(\zeta) = \frac{T - T_\infty}{T_w - T_\infty}, \phi(\zeta) = \frac{C - C_\infty}{C_w - C_\infty}, \chi(\zeta) = \frac{n - n_\infty}{n_w - n_\infty}$$

Where  $\zeta, f'(\zeta), g(\zeta), \theta(\zeta), \phi(\zeta)$  and  $\chi(\zeta)$  depict the similarity variable, dimensionless velocities, non-dimensional temperature, dimensionless concentration and non-dimensional micro-organisms function. Eq (1) is trivially holds by Eq (10), while by applying Eq. (10) into

Eqs. (2)-(9) yield

$$2f''' - \lambda f' + 2ff'' - f'^2 + g^2 - Frf'^2 + \Gamma(\theta - Nr\phi - Nc\chi) = 0 \tag{11}$$

$$2g'' - \lambda g + 2fg' - 2f'g - Frg^2 = 0 \tag{12}$$

$$\frac{1}{Pr^{m+2}} \tag{13}$$

$$\phi'' + scf\phi' + \frac{Nt}{Nb}\theta'' = 0 \tag{14}$$

$$\chi'' + Lbf\chi' - Pe(\phi''(\chi + \omega) + \chi'\phi') = 0 \tag{15}$$

$$f(0) = 0, f'(0) = \alpha f''(0), g(0) = 1 + \alpha g'(0), \theta(0) = 1 + \beta \theta'(0), \phi(0) = 1 + \gamma \phi'(0), \chi(0) = 1 + \delta \chi'(0) \tag{16}$$

$$f'(\infty) \rightarrow 0, g(\infty) \rightarrow 0, \theta(\infty) \rightarrow 0, \phi(\infty) \rightarrow 0, \chi(\infty) \rightarrow 0 \tag{17}$$

where  $Pr = \frac{\nu}{\alpha_m^*}$  Prandtl number,  $\lambda = \frac{\nu f}{\Omega k^*}$  is porosity factor,  $Nb = \frac{D_B(\rho c)_p(C_w - C_\infty)}{(\rho c)_f \nu}$  is Brownian movement,  $Nt = \frac{(\rho c)_p D_T (T_w - T_\infty)}{(\rho c)_f \nu T_\infty}$  thermophoresis coefficient,  $\sigma = \frac{Q_o}{2\Omega(\rho c)_f}$  heat sink/source factor,  $Sc = \frac{\nu}{D_B}$  Schmidt number,  $Lb = \frac{\alpha}{D_m^*}$  is Lewis number,  $Pe = \frac{bW_c}{\nu}$  is Peclet number,  $Fr = \frac{c_b}{k^{\frac{1}{2}}}$  is Forchheimer number,  $\Gamma = \frac{g\beta(1-C_\infty)(T_w - T_\infty)}{r\Omega^2}$  is mixed convection factor,  $Nr = \frac{(\rho_p - \rho_f)(C_w - C_\infty)}{\beta(1-C_\infty)(T_w - T_\infty)}$  Buoyancy ratio coefficient,  $Nc = \frac{\gamma(\rho_m - \rho_f)(n_w - n_\infty)}{\beta(1-C_\infty)(T_w - T_\infty)}$  bio-convection Rayleigh number. Velocities, thermal, concentration microorganism slip parameters are  $\alpha = L'_1 \left( \frac{2\Omega}{\nu} \right)^{\frac{1}{2}}, \beta = L'_2 \left( \frac{2\Omega}{\nu} \right)^{\frac{1}{2}}, \gamma = L'_3 \left( \frac{2\Omega}{\nu} \right)^{\frac{1}{2}}$  and  $\delta = L'_4 \left( \frac{2\Omega}{\nu} \right)^{\frac{1}{2}}$  respectively. The dimensionless forms of skin frictions coefficients  $\sqrt{Re_r} C_f = f''(0), \sqrt{Re_r} C_g = g'(0)$ , Nusselt number  $\frac{Nu}{\sqrt{Re_r}} = -\theta'(0)$ , Sherwood number  $\frac{Sh}{\sqrt{Re_r}} = -\phi'(0)$  and motile number  $\frac{Nn}{\sqrt{Re_r}} = -\chi'(0)$ , where  $Re_r = \frac{2r(r\Omega)}{\nu}$  represents the Reynolds number.

In order to utilize the shooting method, the system of first order differential equations is attained:

$$\begin{aligned} y_1' &= y_2 \\ y_2' &= y_3 \\ y_3' &= 0.5 \left[ y_2^2 - 2y_1y_3 - y_4^2 + \lambda y_2 + Fr y_2^2 - \Gamma(y_6 - Nr y_4 - Nc y_{10}) \right] \\ y_4' &= y_5 \\ y_5' &= 0.5 \left[ \lambda y_4 - 2y_1y_5 + 2y_2y_4 + Fr y_4^2 \right] \\ y_6' &= y_7 \\ y_7' &= -Pr \left[ y_1y_7 + Nb y_7 y_9 + Nt y_7^2 + \sigma y_8 \right] \\ y_8' &= y_9 \\ y_9' &= -Sc y_1 y_9 - \left( \frac{Nt}{Nb} \right) y_7^2 \\ y_{10}' &= y_{11} \\ y_{11}' &= -Lb y_1 y_{11} + Pe \left[ (y_{10} + \omega) y_9' + y_{11} y_9 \right] \end{aligned} \tag{18}$$

Table 1 Numerical data of  $-\chi'(0)$  for varying different parameters

| $Fr$ | $\lambda$ | $Lb$ | $\beta$ | $\gamma$ | $Nt$ | $Nb$ | $\omega$ | $Pr$ | $Pe$ | $-\chi'(0)$ |
|------|-----------|------|---------|----------|------|------|----------|------|------|-------------|
| 0.0  |           |      |         |          |      |      |          |      |      | 0.3918      |
| 0.4  | 0.2       | 1.0  | 0.3     | 0.3      | 0.1  | 0.3  | 1.0      | 1.0  | 1.0  | 0.3708      |
| 0.8  |           |      |         |          |      |      |          |      |      | 0.3528      |
|      | 0.1       |      |         |          |      |      |          |      |      | 0.4036      |
| 0.2  | 0.4       |      |         |          |      |      |          |      |      | 0.3369      |
|      | 1.0       |      |         |          |      |      |          |      |      | 0.2270      |
|      |           | 2.0  |         |          |      |      |          |      |      | 0.5092      |
|      |           | 3.0  |         |          |      |      |          |      |      | 0.5831      |
|      |           | 4.0  |         |          |      |      |          |      |      | 0.6395      |
|      |           |      | 0.1     |          |      |      |          |      |      | 0.3816      |
|      |           |      | 0.5     |          |      |      |          |      |      | 0.3801      |
|      |           |      | 1.0     |          |      |      |          |      |      | 0.3785      |
|      |           |      |         | 0.1      |      |      |          |      |      | 0.3901      |
|      |           |      |         | 0.5      |      |      |          |      |      | 0.3724      |
|      |           |      |         | 1.0      |      |      |          |      |      | 0.3543      |
|      |           |      |         |          | 0.0  |      |          |      |      | 0.4109      |
|      |           |      |         |          | 0.4  |      |          |      |      | 0.2927      |
|      |           |      |         |          | 0.8  |      |          |      |      | 0.1958      |
|      |           |      |         |          |      | 0.4  |          |      |      | 0.3914      |
|      |           |      |         |          |      | 0.8  |          |      |      | 0.4089      |
|      |           |      |         |          |      | 1.0  |          |      |      | 0.4132      |
|      |           |      |         |          |      |      | 0.2      |      |      | 0.4171      |
|      |           |      |         |          |      |      | 0.5      |      |      | 0.5275      |
|      |           |      |         |          |      |      | 1.0      |      |      | 0.7162      |
|      |           |      |         |          |      |      |          | 2.0  |      | 0.3490      |
|      |           |      |         |          |      |      |          | 3.0  |      | 0.3307      |
|      |           |      |         |          |      |      |          | 5.0  |      | 0.3097      |
|      |           |      |         |          |      |      |          |      | 2.0  | 0.5384      |
|      |           |      |         |          |      |      |          |      | 3.0  | 0.6758      |
|      |           |      |         |          |      |      |          |      | 4.0  | 0.8037      |

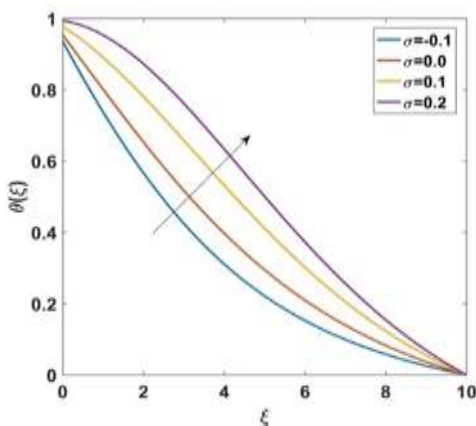


Fig. 1 Sketch of  $\sigma$  on  $\theta(\zeta)$

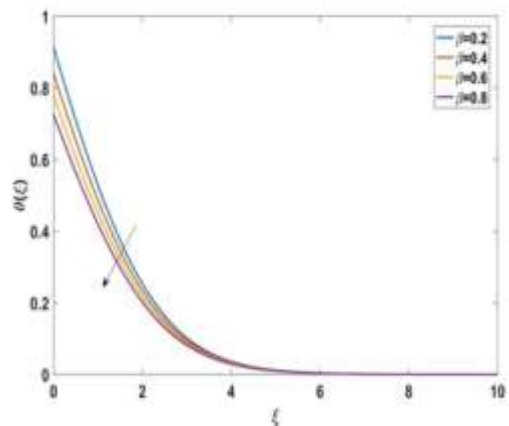


Fig. 2 Sketch of  $\beta$  on  $\theta(\zeta)$

Subject to the non-dimensional boundary conditions are

$$\begin{aligned}
 y_1(0) = 0, y_2(0) = \alpha y_3(0), \\
 y_4(0) = 1 + \alpha y_5(0), y_6(0) = 1 + \beta y_7(0), \\
 y_8(0) = 1 + \gamma y_9(0), y_{10}(0) = 1 + \delta y_{11}(0) \quad (19) \\
 \text{as } \zeta \rightarrow 0
 \end{aligned}$$

$$\begin{aligned}
 y_2(\infty) \rightarrow 0, y_4(\infty) \rightarrow 0, y_6(\infty) \rightarrow 0, \\
 y_8(\infty) \rightarrow 0, y_{10}(\infty) \rightarrow 0 \text{ as } \zeta \rightarrow \infty \quad (20)
 \end{aligned}$$

For the residual of continuous outcomes, the faults control and mesh selection points are utilized for all the calculations.

### 3. Analytical procedure

The presentation of this section is to high light commitment of different physical parameters like heat sink/source parameter,  $\beta$  thermal, Brownian number  $Nb$ , thermophoresis parameter  $Nt$ ,  $\gamma$  concentration, Peclet number  $Pe$ , bioconvected Lewis number  $Lb$ ,  $\delta$  micro-organism on concentration  $\phi$  and density of motile micro-organism  $\chi$  distributions. Table 1 present data of motile microorganism density for varying  $Fr, \lambda, Nb, Nt, \beta, Sc, Pr, Pe, Lb, \omega$  and  $\gamma$ . Impact of heat generation  $\sigma$  on temperature  $\theta$  is displayed in Fig. 1. We noted that by increasing the values of  $\sigma$ , temperature  $\theta$  and thermal layer

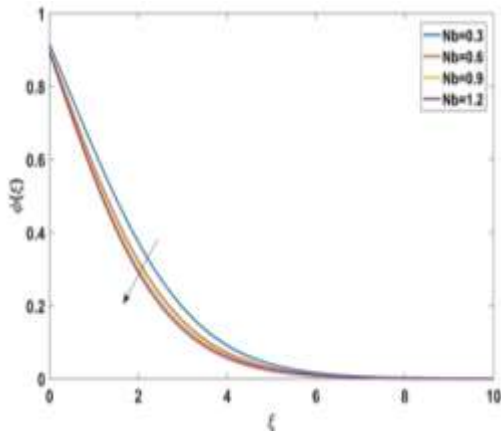


Fig. 3 Sketch of  $Nb$  on  $\phi(\zeta)$

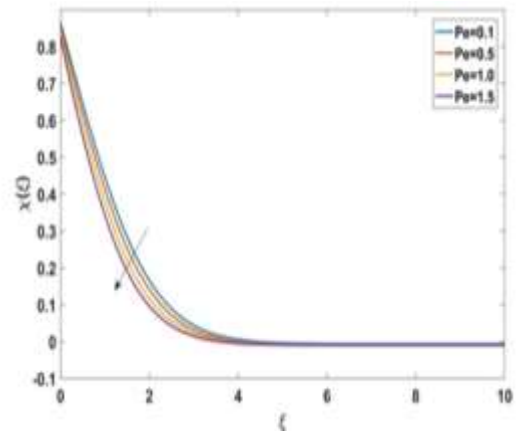


Fig. 6 Sketch of  $Pe$  on  $\chi(\zeta)$

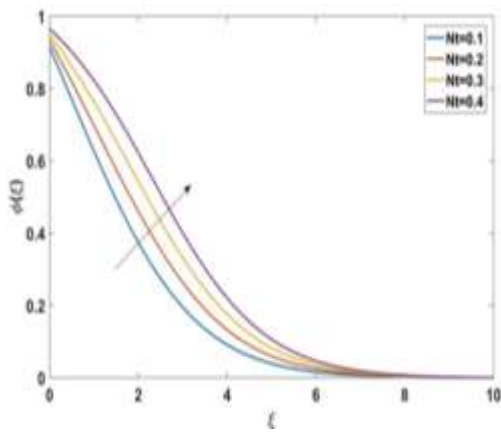


Fig. 4 Sketch of  $Nt$  on  $\phi(\zeta)$

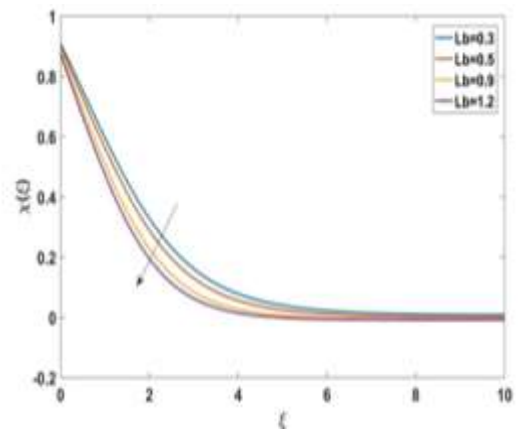


Fig. 7 Sketch of  $Lb$  on  $\chi(\zeta)$

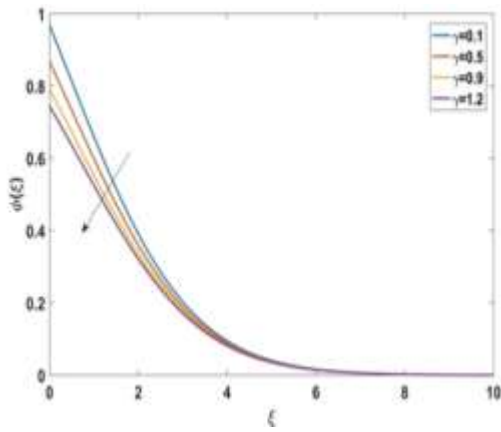


Fig. 5 Sketch of  $\gamma$  on  $\phi(\zeta)$

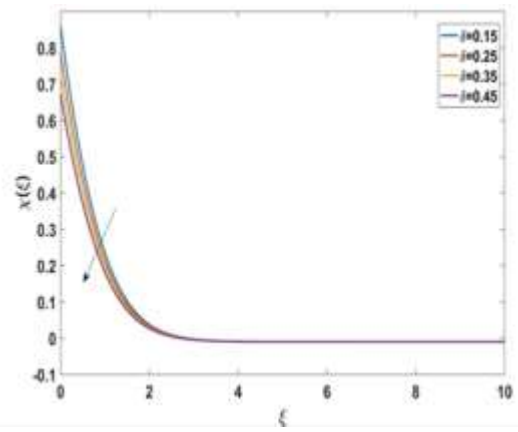


Fig. 8 Sketch of  $\delta$  on  $\chi(\zeta)$

shows expanding behavior. Fig. 2 demonstrates the differing of thermal slip coefficient  $\beta$  when utilized on temperature  $\theta$ . Higher estimations of  $\beta$ , both the temperature  $\theta$  and thickness of related thermal layer shows diminishing trend. The impact of Brownian motion  $Nb$  is displayed on concentration  $\phi$  in Fig. 3. For larger estimations of  $Nb$  both the concentration  $\phi$  and thickness of related concentration layer are degraded. We noted physically, a Brownian endeavor to drag the particles to the other direction of the concentration slop, nanoliquid becomes much homogeneous. After that higher concentration

field, weaker the concentration inclination as greater the Brownian movement. Fig. 4 is prepared to check the curves of concentration  $\phi$  for distinct values of  $Nt$ . It is clearly observed that for higher thermophoretic parameter implies the larger curves of concentration  $\phi$ . For this purpose the nanoparticles are blend in base fluid according to modern science. This phenomenon is occur because migration of nanoparticles from hotter to colder surface far away from the surface. Fig. 5 represents the effect of solutal slip parametry on concentration  $\phi$ . It is visualized that for distinct values of  $\gamma$  exhibit diminishing behavior for

concentration  $\phi$ . The influence of Peclet number  $Pe$  is shown on motile microorganism in Fig. 6. It is noted that for distinct values of  $Pe$ , microorganism  $\chi$  decreases. Reason behind this enhancement in  $Pe$  yields the increment in cell- swimming speed which cause the diminution in gyro-tactic micro-organisms thickness. Fig. 7 shows the impact of bio-convected Lewis number  $Lb$  on microorganism  $\chi$ . The decreasing behavior of  $\chi$  is noted for larger values of  $Lb$ . This is due to less diffusivity of gyro-tactic micro-organisms. The less diffusivity takes place when values of  $Lb$  is increases as a result microorganism  $\chi$  is retarded. The microorganism slip constraint  $\delta$  produce weaker microorganism  $\chi$  as displayed in Fig. 8.

#### 4. Conclusions

Nanoliquids have acquired enormous importance in the current years because of their potential uses, not only as an enhancement of energy transfer but also their immense attention in applications like recovery of fuel and drug delivery. Therefore, the current communication scrutinized the 3D Darcy Forchheimer nanofluid flow due to porous rotatable disk with gyrotactic microorganism and heat source/sink. Thermophoretic and Brownian motion along mass and transfer of heat are also considered. Slip conditions of velocities, temperature, mass and microorganism density are incorporated. For non-dimensional, we use the appropriate variables to handle the modeled equations. A shooting scheme is imposed to obtain the approximate solutions. The reduction is observed for larger like heat sink/source parameter,  $\beta$  thermal, Brownian number  $Nb$ , thermophoresis parameter  $Nt$ ,  $\gamma$  concentration, Peclet number  $Pe$ , bioconvected Lewis number  $Lb$ ,  $\delta$  microorganism on concentration  $\phi$  and density of motile microorganism  $\chi$  distributions.

#### Acknowledgement

This study is supported via funding from Prince Satam bin Abdulaziz University project number (PSAU/2023/R/1444)

#### References

- Abdulrazzaq, M.A., Fenjan, R.M., Ahmed, R.A. and Faleh, N.M. (2020), "Thermal buckling of nonlocal clamped exponentially graded plate according to a secant function based refined theory", *Steel Compos. Struct.*, **35**(1), 147-157. <https://doi.org/10.12989/scs.2020.35.1.147>.
- Agranat, V.M. (1988), "Effect of pressure gradient on friction and heat transfer in a dusty boundary layer", *Fluid Dyn.*, **23**, 729-732. <http://doi.org/10.1007/BF02614150>.
- Akbaş Ş.D. (2017a), "Free vibration of edge cracked functionally graded microscale beams based on the modified couple stress theory", *Int. J. Struct. Stabil. Dyn.*, **17**(3), 1750033.
- Akbaş, Ş.D. (2016a), "Forced vibration analysis of viscoelastic nanobeams embedded in an elastic medium", *Smart Struct. Syst.*, **18**(6), 1125-1143. <https://doi.org/10.12989/sss.2016.18.6.1125>.
- Akbaş, Ş.D. (2016b), "Analytical solutions for static bending of edge cracked micro beams", *Struct. Eng. Mech.*, **59**(3), 579-599. <https://doi.org/10.12989/sem.2016.59.3.579>.
- Akbaş, Ş.D. (2017b), "Forced vibration analysis of functionally graded nanobeams", *Int. J. Appl. Mech.*, **9**(7), 1750100. <https://doi.org/10.1142/S1758825117501009>.
- Akbas, S.D. (2018), "Forced vibration analysis of cracked functionally graded microbeams", *Adv. Nano Res.*, **6**(1), 39-55. <https://doi.org/10.12989/anr.2018.6.1.039>.
- Akgoz, B. and Civalek, O. (2011), "Nonlinear vibration analysis of laminated plates resting on nonlinear two-parameters elastic foundations", *Steel Compos. Struct.*, **11**(5), 403-421. <https://doi.org/10.12989/scs.2011.11.5.403>.
- Al-Maliki, A.F., Ahmed, R.A., Moustafa, N.M. and Faleh, N.M. (2020), "Finite element based modeling and thermal dynamic analysis of functionally graded graphene reinforced beams", *Adv. Comput. Des.*, **5**(2), 177-193. <https://doi.org/10.12989/acd.2020.5.2.177>.
- Baaskaran, N., Ponappa, K. and Shankar, S. (2018), "Assessment of dynamic crushing and energy absorption characteristics of thin-walled cylinders due to axial and oblique impact load", *Steel Compos. Struct.*, **28**(2), 179-194. <https://doi.org/10.12989/scs.2018.28.2.179>.
- Batou, B., Nebab, M., Bennai, R., Atmane, H.A., Tounsi, A. and Bouremana, M. (2019), "Wave dispersion properties in imperfect sigmoid plates using various HSDTs", *Steel Compos. Struct.*, **33**(5), 699-716. <https://doi.org/10.12989/scs.2019.33.5.699>.
- Benmansour, D.L., Kaci, A., Bousahla, A.A., Heireche, H., Tounsi, A., Alwabli, A.S., Alhebshi, A.M., Al-ghmady, K. and Mahmoud, S.R. (2019), "The nano scale bending and dynamic properties of isolated protein microtubules based on modified strain gradient theory", *Adv. Nano Res.*, **7**(6), 443-457. <https://doi.org/10.12989/anr.2019.7.6.443>.
- Chakrabarti, K.M. (1974), "Note on boundary layer in a dusty gas", *Am. Inst. Aeronaut. Astronaut. J.*, **12**, 1136-1137. <http://doi.org/10.2514/3.49427>.
- Chamkha, A.J., Abd El-Aziz, M.M. and Ahmed, S.E. "Effects of thermal stratification on flow and heat transfer due to a stretching cylinder with uniform suction/injection", *Int. J. Energy Technol.*, **2**(4), 1-7.
- Chen, J., Zhuang, Y., Fang, H., Liu, W., Zhu, L. and Fan, Z. (2019a), "Energy absorption of foam-filled lattice composite cylinders under lateral compressive loading", *Steel Compos. Struct.*, **31**(2), 133-148. <https://doi.org/10.12989/scs.2019.31.2.133>.
- Chen, W., Ji, C., Alam, M.M. and Xu, D. (2019b), "Flow-induced vibrations of three circular cylinders in an equilateral triangular arrangement subjected to cross-flow", *Wind Struct.*, **29**(1), 43-53. <https://doi.org/10.12989/was.2019.29.1.043>.
- Civalek, Ö. (2017), "Free vibration of carbon nanotubes reinforced (CNTR) and functionally graded shells and plates based on FSDT via discrete singular convolution method", *Compos. Part B Eng.*, **111**, 45-59. <https://doi.org/10.1016/j.compositesb.2016.11.030>.
- Dawar, A., Wakif, A., Thumma, T. and Shah, N.A. (2022), "Towards a new MHD non-homogeneous convective nanofluid flow model for simulating a rotating inclined thin layer of sodium alginate-based Iron oxide exposed to incident solar energy", *Int. Commun. Heat Mass Transf.*, **130**, 105800. <https://doi.org/10.1016/j.icheatmasstransfer.2021.105800>.
- Derakhshandeh, J.F. and Alam, M.M. (2020), "Reynolds number effect on the flow past two tandem cylinders", *Wind Struct.*, **30**(5), 475-483. <https://doi.org/10.12989/was.2020.30.5.475>.
- Ebrahimi, F., Dabbagh, A., Rabczuk, T. and Tornabene, F. (2019), "Analysis of propagation characteristics of elastic waves in heterogeneous nanobeams employing a new two-step porosity-



- dependent homogenization scheme”, *Adv. Nano Res.*, **7**(2), 135-143. <http://doi.org/10.12989/anr.2019.7.2.135>.
- Eltaher, M.A., Almalki, T.A., Ahmed, K.I. and Almitani, K.H. (2019), “Characterization and behaviors of single walled carbon nanotube by equivalent-continuum mechanics approach”, *Adv. Nano Res.*, **7**(1), 39-49. <http://doi.org/10.12989/anr.2019.7.1.039>.
- Iqbal, W., Naeem, M.N., Jalil, M. (2019), “Numerical analysis of Williamson fluid flow along an exponentially stretching cylinder”, *AIP Adv.*, **9**(5), 055118. <http://doi.org/10.1063/1.5092737>.
- Ishak, A., Nazar, R. (2009), “Laminar boundary layer flow along a stretching cylinder”, *Eur. J. Sci. Res.*, **36**(1), 22-29.
- Ishak, A., Nazar, R. and Pop, I. (2008), “Uniform suction/ blowing effect on flow and heat transfer due to stretching cylinder”, *Appl. Math. Mod.*, **32**, 2059-2066. <http://doi.org/10.1016/j.apm.2007.06.036>.
- Khan, M., Malik, R. (2015), “Forced convective heat transfer to Sisko fluid flow past a stretching cylinder”, *AIP Adv.*, **5**(12), 127202. <http://doi.org/10.1063/1.4937346>.
- Khan, Z.A., Shah, N.A., Haider, N., El-Zahar, E.R. and Yook, S.J. (2022), “Analysis of natural convection flows of Jeffrey fluid with Prabhakar-like thermal transport”, *Case Stud. Therm. Eng.*, **35**, 102079. <https://doi.org/10.1016/j.csite.2022.102046>.
- Konch, J., Hazarika, G.C. (2017), “Unsteady Hydro magnetic flow of dusty fluid over a stretching cylinder with variable viscosity and thermal conductivity”, *Int. J. Adv. Sci. Tech.*, **99**, 57-70. <http://doi.org/10.14257/ijast.2017.99.05>.
- Imtiaz, M., Hayat, T. and Alsaedi, A. (2016), “Mixed convection flow of Casson nanofluid over a stretching cylinder with convective boundary conditions”, *Adv. Power Tech.*, **27**(5), 2245-2256. <https://doi.org/10.1016/j.appt.2016.08.011>.
- Mahdy, A. (2015), “Heat transfer and flow of a Casson fluid due to a stretching cylinder with the sores and dufour effects”, *J. Eng. Phys. Therm.*, **88**(4), 928-936. <https://doi.org/10.1007/s10891-015-1267-6>.
- Malik, M.Y., Hussain, A., Salahuddin, T., Awais, M., Bilal, S. and Khan, F. (2016), “Flow of Sisko fluid over a stretching cylinder and heat transfer with viscous dissipation and variable thermal conductivity: A numerical study”, *AIP Adv.*, **6**(4), 045118. <https://doi.org/10.1063/1.4948458>.
- Malik, M.Y., Naseer, M., Nadeem, S., Rehman, A. (2013), “The boundary layer flow of Casson nanofluid over an exponentially stretching cylinder”, *Appl. Nanosci.*, **4**, 869-873. <https://doi.org/10.1007/s13204-013-0267-0>.
- Naseer, M., Malik, M.Y., Nadeem, S., Rehman, A. (2014), “The boundary layer flow of hyperbolic tangent fluid over a vertical exponentially stretching cylinder”, *Alexandria Eng. J.*, **53**, 747-750. <https://doi.org/10.1016/j.aej.2014.05.001>.
- Ramesh, G.K., Madhukesh, J.K., Das, R., Shah, N.A. and Yook, S.J. (2022), “Thermodynamic activity of a ternary nanofluid flow passing through a permeable slipped surface with heat source and sink”, *Waves Random Complex Med.*, 1-21. <https://doi.org/10.1080/17455030.2022.2053237>.
- Rasekh, A., Ganji, D.D., Tavakoli, S., Ehsani, H., Naejee, S. (2014), “MHD flow and heat transfer of dusty fluid over a stretching hollow cylinder with a convective boundary conditions”, *Heat Trans. Asian Res.*, **43**(3), 221-232. <https://doi.org/10.1002/htj.21073>.
- Rebhi, A.D. (2010), “On boundary layer flow of dusty gas from a horizontal circular cylinder”, *Braz. J. Chem. Eng.*, **27**(4), 653-662. <http://doi.org/10.1590/S0104-66322010000400017>.
- Rehman, A. (2015), “Boundary layer flow and heat transfer of micropolar fluid over a vertical exponentially stretching cylinder”, *Appl. Comp. Math.*, **4**(6), 424-430. <http://doi.org/10.11648/j.acm.20150406.15>.
- Sabu, A.S., Wakif, A., Areekara, S., Mathew, A. and Shah, N.A. (2021), “Significance of nanoparticles’ shape and thermo-hydrodynamic slip constraints on MHD alumina-water nanoliquid flows over a rotating heated disk: The passive control approach”, *Int. Commun. Heat Mass Transf.*, **129**, 105711. <https://doi.org/10.1016/j.icheatmasstransfer.2021.105711>.
- Safaei, B., Khoda, F.H. and Fattahi, A.M. (2019), “Non-classical plate model for single-layered graphene sheet for axial buckling”, *Adv. Nano Res.*, **7**, 265-275. <https://doi.org/10.12989/anr.2019.7.4.265>.
- Saffman, P.G. (1962), “On the stability of laminar flow of a dusty gas”, *J. Fluid Mech.*, **13**, 120-128. <https://doi.org/10.1017/S0022112062000555>.
- Salah, F., Boucham, B., Bourada, F., Benzair, A., Bousahla, A. A. and Tounsi, A. (2019), “Investigation of thermal buckling properties of ceramic-metal FGM sandwich plates using 2D integral plate model”, *Steel Compos. Struct.*, **33**(6), 805-822. <https://doi.org/10.12989/scs.2019.33.6.805>.
- Salahuddin, T., Malik, M.Y., Hussain, A., Awais, M., Bilal, S. (2017), “Mixed convection boundary layer flow of Williamson fluid with slip conditions over a stretching cylinder by using Keller-box method”, *Int. J. Nonlinear Sci. Numer. Simul.*, **18**(1), 9-17. <https://doi.org/10.1515/ijnsns.2015.0090>.
- Shadravan, S., Ramseyer, C.C. and Floyd, R.W. (2019), “Comparison of structural foam sheathing and oriented strand board panels of shear walls under lateral load”, *Adv. Comput. Des.*, **4**(3), 251-272. <https://doi.org/10.12989/acd.2019.4.3.251>.
- Shahsavari, D., Karami, B. and Janghorban, M. (2019), “Size-dependent vibration analysis of laminated composite plates”, *Adv. Nano Res.*, **7**(5), 337-349. <https://doi.org/10.12989/anr.2019.7.5.337>.
- Sun, X., Animasaun, I.L., Swain, K., Shah, N.A., Wakif, A. and Olanrewaju, P.O. (2022), “Significance of nanoparticle radius, inter-particle spacing, inclined magnetic field, and space-dependent internal heating: The case of chemically reactive water conveying copper nanoparticles”, *ZAMM*, **102**(4), e202100094. <https://doi.org/10.1002/zamm.202100094>.
- Wang, C.Y. (1988), “Fluid flow due to a stretching cylinder”, *Phys. Fluids*, **31**, 466-468. <https://doi.org/10.1063/1.866827>.
- Wang, C.Y., Ng, C.O. (2011), “Slip flow due to a stretching cylinder”, *Int. J. Non-Lin. Mech.*, **46**, 1191-1194. <https://doi.org/10.1016/j.ijnonlinmec.2011.05.04>.

CC